Optical Fiber Technology 22 (2015) 36–41

Contents lists available at ScienceDirect

Optical Fiber Technology

www.elsevier.com/locate/yofte

Strong power transfer between photonic bandgaps of hybrid photonic crystal fibers

S. Arismar Cerqueira Jr. [a,*], A.R. do Nascimento Jr. [b], I.A.M. Bonomini [a], M.A.R. Franco [c], V.A. Serrão [c], C.M.B. Cordeiro [d]

[a] Laboratory WOCA (Wireless and Optical Convergent Access), National Institute of Telecommunications (Inatel), Av. João Camargo 510, Santa Rita do Sapucaí, MG, Brazil
[b] School of Electrical and Computer Engineering, State University of Campinas, Campinas, SP 13083-852, Brazil
[c] Institute for Advanced Studies, 1 Trevo Coronel Aviador do Amarante, São José dos Campos, SP 1228-001, Brazil
[d] Instituto de Física Gleb Wataghin, UNICAMP, R. Sergio Buarque de Holanda 777, Campinas, SP, Brazil

ARTICLE INFO

Article history:
Received 21 December 2013
Revised 24 September 2014
Available online 2 February 2015

Keywords:
Hybrid PCF
Nonlinear optics
Photonic crystal fibers
Power transfer

ABSTRACT

This work reports the strong nonlinear power transfer between two adjacent photonic bandgaps of hybrid photonic crystal fibers. The nonlinear phenomenon originates from the generation of a resonant radiation in a particular bandgap, which is ensured by launching a femtosecond pulse near the zero-dispersion wavelength of a lower-order adjacent bandgap, where its correspondent soliton is formed. A theoretical description based on fiber dispersion properties and phase-matching conditions is presented to contribute to the interpretation and understanding of the highly efficient energy transference. Furthermore, various experimental results are reported, including the resonant radiation that peaks at 8.5 dB above that of the initial pulse, which represents a significant enhancement in the nonlinear efficiency compared to previous published works in the literature.

1. Introduction

Photonic crystal fibers (PCFs) have been intensively used in the last two decades because of their remarkable and unique optical properties [1]. Contrary to the early days of optical fibers, PCF technology provides new degrees of freedom in terms of light guidance, fabrication techniques and fiber materials and structures. These remarkable advances allow them to yield several interesting and technologically enabling properties, which are superior to the traditional optical fibers in numerous aspects and diverse applications.

For the first time, hybrid PCFs enables light propagation in an optical fiber via two propagation mechanisms simultaneously [2]: total internal reflection and antiresonant effect. These fibers are typically based on an undoped silica core surrounded by a wavelength-scale two-dimensional photonic crystal, which is formed using air holes arranged in a hexagonal pattern and a line of high-index inclusions. The high-index inclusions are composed of germanium rods, which form antiresonance regions and photonic bandgaps. Thus, light at wavelengths that satisfy this condition is guided in the pure silica core.

After its invention in 2006, hybrid PCFs based on different geometries have been proposed and analyzed. For example, L. Xiao et al presented some numerical results of a hybrid PCF with a hexagonal array of high-index rods and a line of air holes [3]. Ould-Agha et al. recently proposed a new structure of one ring of six high-index rods to extend the transmission band by at least 200% [4]. Moreover, hybrid PCFs have been investigated for linear and nonlinear applications such as broadband polarizers [5] optical amplifiers [6] optical sensors [7] soliton generation [8,9] and supercontinuum generation [10,11]. This work presents an analytical description and experimental results on highly efficient power transfer between the second and third photonic bandgaps (PBGs) of different hybrid PCFs.

2. Hybrid photonic crystal fibers

Light guidance in conventional optical fibers is based on two concentric regions with different doping levels: the core and cladding regions, whereas in PCFs, it is based on subtle variations in the refractive index by corralling light in a microscopic and periodic array of air holes. This property makes the cladding index strongly wavelength-dependent, which enables new degrees of freedom in terms of light propagation. Considering the propagation mechanism of light guidance in PCFs, there are basically four types of

* Corresponding author.
E-mail address: arismar@inatel.br (S. Arismar Cerqueira Jr.).

http://dx.doi.org/10.1016/j.yofte.2015.01.006
1068-5200/

PCFs: index-guiding PCF based on the modified total internal reflection (TIR); hollow-core PCF, which enables light propagation in air using the PBG effect; all-solid PBGF based on the antiresonant effect, which is central to the PBG effect in these fibers; hybrid PCF, which provides light guidance using both propagation mechanisms simultaneously; Kagomé PCF, which guides light via inhibited coupling between the core and cladding modes.

Particularly, hybrid PCFs are composed of air holes and germanium-doped silica rods, which are disposed around an undoped silica core, as shown in Fig. 1a. The air holes are arranged in a hexagonal pattern as in the index-guiding PCFs, whereas the high-index rods replace a single row of air holes along one of the PCF axes and form a one-dimensional PBG in this direction. Compared with the traditional PCFs, one more design parameter must be included: the rod diameter D. Light guidance in hybrid PCFs occurs only in restricted bands of wavelength, which coincide with the photonic bandgaps because both propagation mechanisms are responsible for light confinement in the hybrid PCF core [2]. The possibility of exploiting the TIR and photonic bandgap effect in a unique fiber enables nonlinear fiber-optic experiments in new dispersion regimes.

The relevant properties of hybrid PCFs, such as dispersion and nonlinearity, are closely related to their modal intensity patterns [1,2]. The pattern of the hybrid-PCF modes are believed to arise when the more dispersive modes of the high-index rods intersect with the mode of a standard index-guiding PCF, which causes anti-crossings. The hybrid modes are linear combinations of the core mode with the corresponding high-index rod mode, which is the closest one to be resonant.

The hybrid PCF design has been realized using the PCFDT (Photonic Crystal Fiber Design Tool) [12], which is our numerical tool based on the Finite Element Method (FEM). The main goal was to obtain hybrid PCFs with a zero dispersion wavelength (λ_0) near 805 nm, which is the central wavelength of our femtosecond system. The selected design parameters of the three hybrid PCFs for the nonlinear experiments are summarized in Table 1. The Ge rods present a gradual refractive index and maximum step $\Delta n = 2.03\%$. All fibers were fabricated at the University of Bath in the UK.

A PCF-based supercontinuum source, which extends from 450 to 1700 nm, was launched at the hybrid PCFs' input to measure their photonic. Fig. 1b shows the transmission spectrum of fiber B, which was obtained with a one-meter-long sample. It shows three bandgaps and low-attenuation windows in the silica transparency wavelength range: the 1st PBG is from 1060 to 1350 nm; the 2nd PBG is centered at approximately 750 nm; the 3rd PBG is at approximately 530 nm. The positions of the 2nd and 3rd PBGs are favorable to optimize their power transfer. Fibers A and C have notably similar transmission properties with fiber B; they also provide three PBGs in the silica transparency window. However, the PBGs are translated to shorter and longer wavelength ranges because as soon as the high-index diameter is increased, the PBG edges are shifted to longer wavelengths. Consequently, an opposite effect occurs when the rod diameter is decreased, i.e., the PBG edges are moved to shorter wavelengths.

The numerical simulations of the chromatic dispersion in the second PBG for the three hybrid PCFs are presented in Fig. 2. As

Table 1
Design parameters of the hybrid PCFs in micrometers (μm).

Fiber name/ parameter	Air hole diameter	Inter-hole spacing	Rod diameter
Fiber A	1.61	3.75	2.70
Fiber B	1.76	4.04	2.81
Fiber C	1.85	4.31	2.96

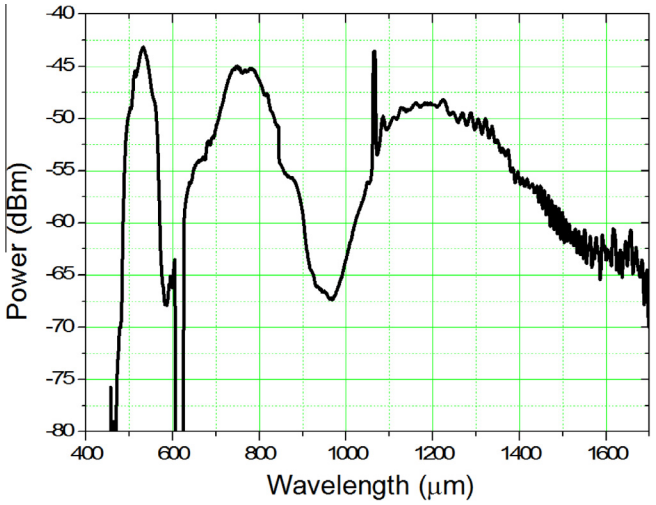

Fig. 1b. Measured transmission spectrum of Fiber B. The bandgaps are the three low-attenuations windows: the 1st PBG is from 1060 to 1350 nm; the 2nd PBG is centered at approximately 750 nm; the 3rd PBG is at approximately 530 nm.

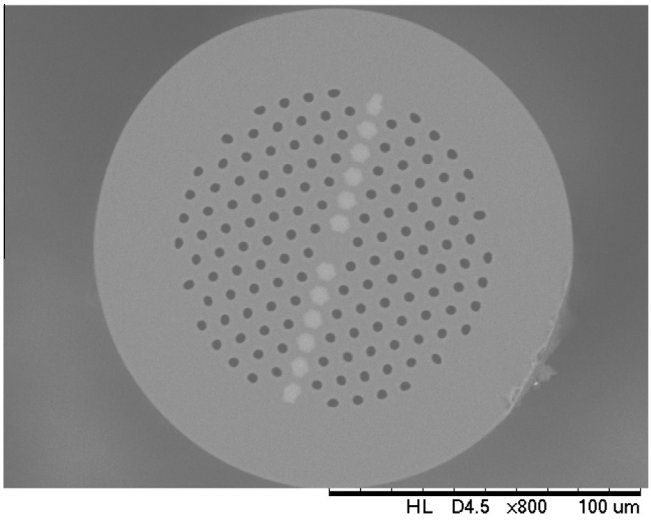

Fig. 1a. Hybrid photonic crystal fiber: the air holes are arranged in a hexagonal pattern as in the index-guiding PCFs, whereas the high-index rods replace a single row of air holes along one of the PCF axes. SEM image.

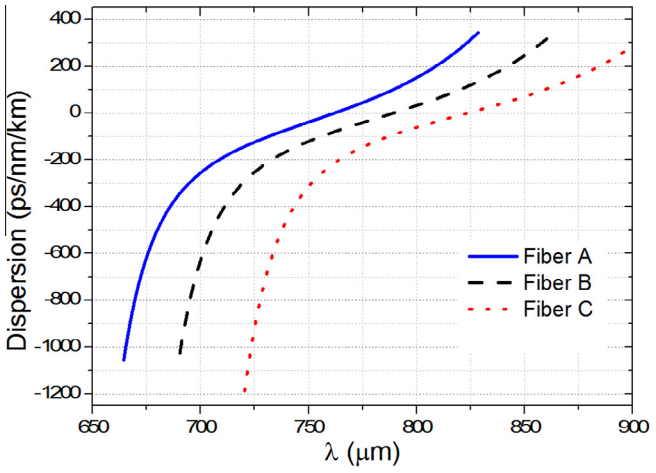

Fig. 2. Numerical simulations of the chromatic dispersion of the three hybrid PCFs in the nonlinear experiments.

expected, the zero dispersion wavelengths of fibers A and C are positioned at shorter and longer wavelengths than that of fiber B, respectively. This phenomenon can be explained as follows. The cladding-state bandgaps are the wavelength ranges among the cut-offs of the higher-order guided modes of an isolated rod (crossing points of the LP mode lines with the cladding refractive index). The transmission maxima result from the antiresonant wavelengths that experience destructive interference in the high-index layer; thus, light is confined to the low-index core [2]. As soon as the Ge rod is increased, both the PBG edges and the zero dispersion are shifted to longer wavelengths. Alternatively, the dispersive characteristics of the bandgap modes can be described using the Kramers–Kronig model [13].

The zero-dispersion wavelengths in the second bandgap are 761, 791 and 823 nm for fibers A, B and C, respectively. Therefore, fiber B is the most promising fiber for the nonlinear experiments because it provides the closest λ_0 to the central wavelength of our femtosecond system.

3. Power transfer theory

Optical solitons or solitary waves are formed as a result of the interplay between the fiber dispersive and nonlinear effects, which eliminates the effects of dispersion. Solitons are caused by the nonlinear effect of Self-Phase Modulation (SPM), which implies that the electric field of the wave changes the observed index of refraction of the wave (Kerr effect). SPM causes a redshift at the leading edge of the pulse. Solitons occur when this shift is canceled because of the blueshift at the leading edge of a pulse in an anomalous-dispersion region, which results in a pulse that maintains its shape in both frequency and time.

The word "soliton" refers to special types of wave packets that can propagate undistorted over notably long distances. In other words, they are light pulses that propagate without dispersion, although the medium through which they travel is naturally dispersive. The PCF technology provides a wonderful context for soliton propagation because it provides unprecedented control over both nonlinear response and fiber dispersion. Therefore, PCF-based solitons can be useful in real-world applications.

For a powerful laser pulse that propagates in an optical fiber, when a significant part of its spectrum experiences anomalous group velocity dispersion (GVD), the pulse usually disintegrates into a mixture of solitons and dispersive waves. The power transfer between photonic bandgaps of hybrid PCFs is based on the soliton propagation in the pumping PBG and the generation of a resonant radiation in an adjacent PBG [9]. This nonlinear phenomenon can be properly analyzed by solving the nonlinear Schrödinger equation using the inverse scattering method. Then, it is possible to prove that the width and peak power of the fundamental soliton and its correspondent dispersive waves are related to the input pulse width and peak power [14].

A high-order soliton remains intact only if all of its constituent fundamental solitons travel with an identical group velocity [15]. Particularly, many high-order dispersive and nonlinear effects become important when a femtosecond pulse propagates through a highly nonlinear fiber. In 2008, our group first demonstrated the appearance of a blue-shifted dispersive wave in a different photonic bandgap, which is called the resonant radiation (RR) or non-solitonic radiation [9]. A fundamental soliton sheds its energy to a dispersive wave at a specific frequency whenever a third-order dispersion (TOD) perturbs it. Theoretically, dispersive waves are linear waves that can propagate in any dispersive medium. However, they are only experimentally observed under appropriate phase conditions [9]. This section aims to propose an analytical description to contribute towards the interpretation and understanding of the nonlinear power transfer between two adjacent PBGs.

Fiber dispersion is important in the propagation of short pulses because different spectral components associated with the pulse travel at different speeds, which are given by the ratio between the light velocity and the fiber refractive index as a function of the wavelength. Mathematically, the fiber dispersion effect is accounted for by expanding the mode-propagation constant β in a Taylor series about the frequency at which the pulse spectrum is centered [15]. In index-guiding fibers, β is expanded up to the third-order dispersion coefficient. The same approximation can be assumed for PCFs based on the photonic bandgap effect, which include hybrid PCFs, if the pulse propagation is within the bandgaps.

The parameter $k(\lambda)$ represents the moving-frame measure of the linear propagation constant at wavelength λ compared to its value at the soliton central wavelength. Because the nonlinear experiments are performed in the bandgap regions, let us consider the real function $k(\lambda)$ that is expanded to the third-order dispersion coefficient as in the index-guiding fibers:

$$k(\lambda) = \frac{2\pi^2 c^2 \beta_2}{\lambda_0^2}\left(\frac{\lambda_0 - \lambda}{\lambda}\right)^2 + \frac{4}{3}\frac{\pi^3 c^3 \beta_3}{\lambda_0^3}\left(\frac{\lambda_0 - \lambda}{\lambda}\right)^3 \quad (1)$$

The zero of (1), which is denoted as λ^*, where the wavelength of the resonant radiation is generated in a different bandgap, is calculated using:

$$\lambda^* = \frac{\lambda_0}{1 - \frac{\beta_2}{2\pi c \beta_3}\lambda_0} \quad (2)$$

Numerical simulations demonstrate that hybrid PCFs, as well as photonic bandgap fibers (PBGFs) [11,16], always provide positive β_3. If β_2/β_3, the wavelength of the resonant radiation is shorter than the zero dispersion wavelength of the correspondent PBG ($\lambda^* < \lambda_0$). Therefore, Eq. (2) satisfies the dispersion properties of the second PBG of the three hybrid PCFs in the nonlinear experiments: β_3 is always positive, and β_2 is negative ($D > 0$) over most parts of our femtosecond source spectrum. In particular, for fibers A and B, β_2 and β_3 have opposite signs at its central wavelength (805 nm). Using (2), it is possible to analyze the nonlinear power transfer from a lower-order to a higher-order bandgap, i.e., a generation of a blue-shifted resonant radiation. This paper focuses on the power transfer from the 2nd to the 3rd PBG.

The RR frequency ω_{RR} is governed by the phase matching between the soliton and the low-amplitude linear waves. In other words, the soliton wavenumber β_S should be equal to the fiber linear dispersion curve β at the frequency ω_{RR} ($\beta_S(\omega_{RR}) = \beta(\omega_{RR})$). The nonlinear phase-shift is used to predict the location of dispersive wave emission [17]. Inconsistencies between the theoretical prediction and experimental results are frequently attributed to the uncertainty in the fiber dispersion properties. However, Austin et al. demonstrated that even in simulations, significant inconsistency occurs, particularly at high powers levels, where the dispersive wave generation is the most efficient [11]. They proved that the dispersive wave generation is nonetheless properly described using a fundamental soliton-like state if a redshift caused by higher-order dispersion in considered.

The radiation condition between the soliton and the emitted radiation [18] is satisfied at the wavelength λ_{RR}, which is approximately given by $k(\lambda) = \gamma(\omega_S)P_S/2$. The nonlinear coefficient for the hybrid PCFs is approximately $\gamma = 7.5\ W^{-1}\ km^{-1}$. Fig. 3 presents a phase-matching analysis as a function of the fiber chromatic dispersion properties in the 2nd PBG by varying the chromatic dispersion parameter D at 805 nm and maintaining a constant S_0. The light yellow regions illustrate the bandgaps of fiber B. When the dispersion is increased, it becomes more difficult to generate RR

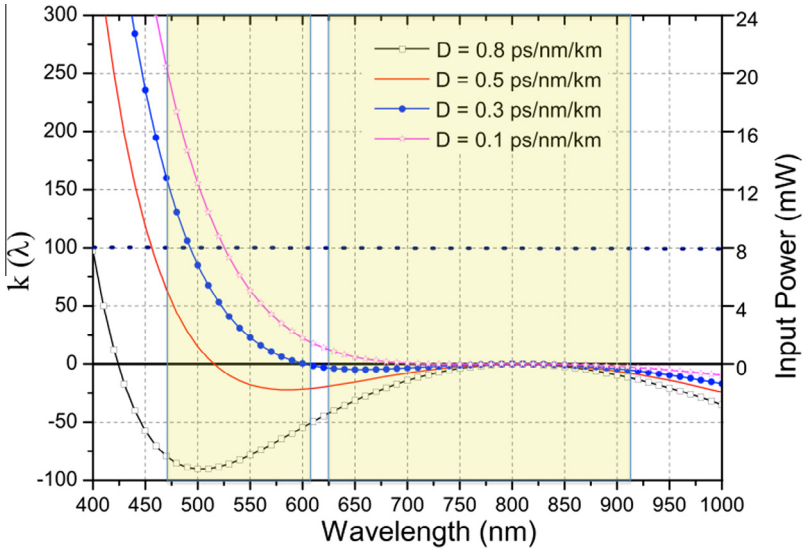

Fig. 3. Analytical description of phase matching as a function of the chromatic dispersion properties in the 2nd PBG.

in the wavelength range of the 3rd PBG because it is shifted to shorter wavelengths. For example, at an average power of $P_S = 8$ mW (typical value in the experiments), λ_{RR} is experimentally observed for D of 0.1 and 0.3 ps/nm/km. However, for the other two cases, it is generated at a wavelength outside the bandgap and does not have sufficient power to be experimentally observed. Therefore, Fig. 3 demonstrates that the location of the minimum point from the $k(\lambda)$ curves determines the chances of generating RR in the next bandgap. The interval $[\lambda_2^* \lambda_0]$, is obtained by finding the wavelength where the derivative of (2) vanishes:

$$\lambda_{min} = \frac{\lambda_0}{1 - \frac{\beta_2}{3\pi c \beta_3}} \tag{3}$$

This simple equation can be efficiently applied to design hybrid PCFs with dispersion properties that enable power transfer between bandgaps using the resonant radiation emitted by a soliton in an adjacent bandgap. Therefore, the presented analytical description can be used as guidelines to develop new hybrid PCFs that can further enhance the nonlinear efficiency and ensure that the power transfer occurs at the required wavelength for a specific application.

4. Experimental results

This section presents experimental results on highly efficient power transfer between bandgaps, which strongly depends on the input peak power, fiber length, chromatic dispersion and nonlinear properties. The experimental setup, which is illustrated in Fig. 4a, was used to demonstrate the nonlinear energy transference and experimentally analyze its efficiency as a function of the fiber dispersion and length. It has the following pieces of equipment: a femtosecond system centered at 805 nm with a pulse duration of 40 fs and a repetition rate of 1 kHz; a variable attenuator; two polarizers; a half-wave plate; a few objective lens; a collecting fiber; an optical spectrum analyzer. The variable attenuator and a half-wave plate were placed at the fiber input to adjust the optical power and rotate the polarization state, respectively. The optical polarizers were used to identify the fiber slow and fast axes to enhance the nonlinear efficiency. This procedure was necessary because of high birefringence from hybrid PCFs, which originates from the stress induced by germanium-doped silica rods [19].

The three hybrid PCFs were fabricated using the same preform and provide the 2nd PBG around the pump wavelength range and the 3rd one in the visible range. Fig. 5 reports the output spectra that were obtained using the 5.0 m fiber samples at an average pump power of 8.0 mW. The initial pulse was broadened around the pump wavelength because of the Self-Phase Modulation (SPM). A nonlinear interaction between the 2nd and 3rd PBGs, which generated a soliton in the 2nd PBG and created RR (λ^*) in the 3rd PBG at the following wavelengths: 478 nm (fiber A); 493 nm (fiber B); 561 nm (fiber C). As expected, a larger Ge rod corresponds to a longer RR wavelength. At these wavelengths, the RR phase velocity matches the soliton phase velocity. The frequency shift between them is a temporal analog of the angle where the Cherenkov radiation is emitted by charged particles in a bulk medium [15]. Furthermore, it is important to notice that the best nonlinear efficiency was obtained for fiber B, where the RR has a higher peak than the initial pulse (approximately 6.6 dB). The efficiency of this fiber is most enhanced because of the closest proximity of its λ_0 to the femtosecond pulse central wavelength.

The next step was to experimentally analyze the nonlinear efficiency as a function of the power variation ΔP between the RR

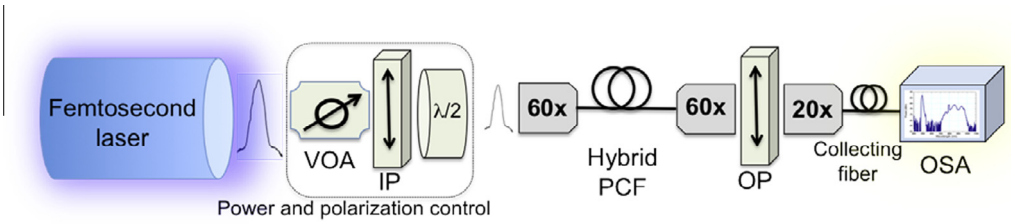

Fig. 4. Experimental setup: VOA – variable optical attenuator; IP – input polarizer; OP – output polarizer; OSA – optical spectrum analyzer.

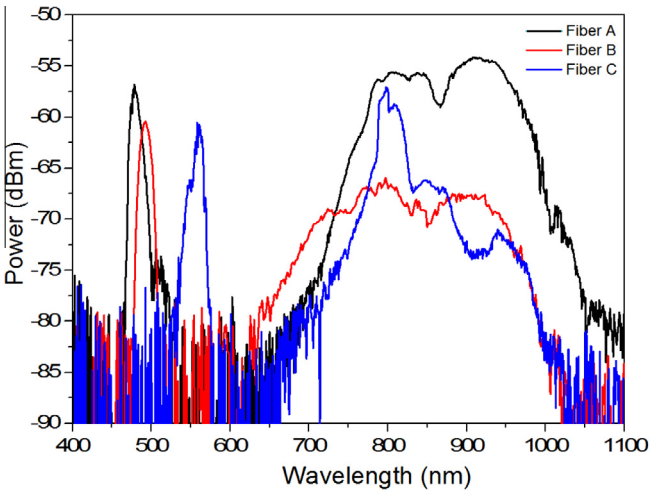

Fig. 5. Power transfer between bandgaps for three different hybrid PCFs.

spectral intensity and the pumping pulse intensity as a function of the fiber length. The optical input power and polarization properties were maintained constant. The nonlinear interaction becomes much more intense, i.e., $\Delta P > 5$ dB, for the lengths above 3 m. This parameter reaches 8.5 dB for 6 m, as shown in Fig. 6, which was the longest remained fiber piece, because the nonlinearity is accumulated when the fiber length increases, and more energy is consequently transferred from the 2nd PBG to the 3rd PBG, which produces a strong power transfer between the bandgaps. The nonlinear power transfer was significantly improved compared to our previous works because in the current work, the spectral intensity of RR is 8.5 dB higher than that of the initial pulse, whereas it was 2.7 dB below it in [9] and 5.5 dB above it in [20]. The efficiency is mainly enhanced because of three reasons: fiber quality and precision; the fiber lengths are a few meters; increase in the peak power level. Improvements of the fiber fabrication process enable proper control of the zero-dispersion wavelength position in the third bandgap to make it notably close to the pumping source wavelength. In addition, the new hybrid PCFs provide more axial uniformity, which enables constant phase matching over the fiber propagation length. The use of longer fiber pieces of up to six meters and higher power levels allow us to increase the figure of merit from the nonlinear process, which is the product between the effective length and the intensity (power per unit of area).

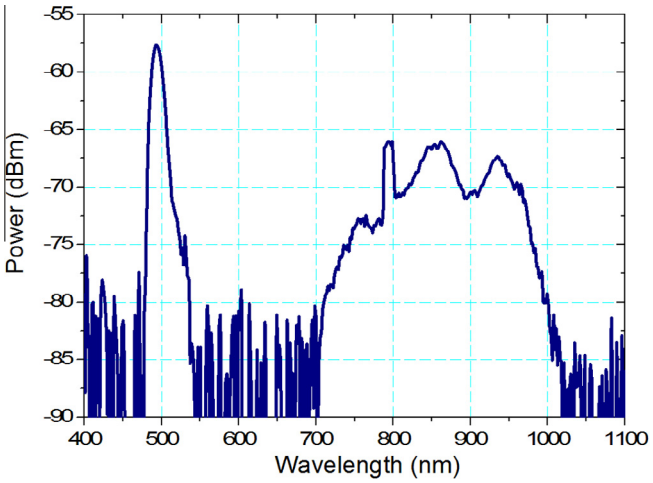

Fig. 6. Strong power transfer between the second and the third bandgaps of fiber B.

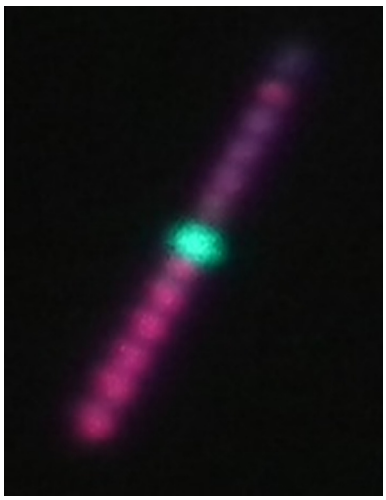

Fig. 7. Photograph of fiber B output for illustrating the nonlinear power transfer between adjacent photonic bandgaps: bluish green light generated in the third PBG. (For interpretation of the references to color in this figure legend, the reader is referred to the web version of this article.)

Finally, a traditional digital camera was used to obtain a near-field image at the output of fiber B to illustrate the strong power transfer between its adjacent bandgaps. In the photograph in Fig. 7, one clearly observes intense bluish green light propagation in the visible range in the hybrid PCF core. As previously mentioned, a part of the initial pulse energy at 805 nm (infrared region), which was launched in the 2nd bandgap, was converted to visible light at 493 nm in the 3rd photonic bandgap.

5. Conclusions

In conclusion, the strong nonlinear power transfer between bandgaps of hybrid photonic crystal fibers was reported. The phenomenon originates from the soliton formation in the second PBG and the generation of a dispersive wave in the third PBG. The dispersive wave is called the "resonant radiation" and is blue-shifted to a specific wavelength, which originates from the third-order dispersion perturbation. A photograph of the fiber output illustrates the emission of notably strong RR in the visible region. In the best case, it appears in bluish green and peaks at 8.5 dB above that of the initial pulse. This result represents the most efficient nonlinear power transfer between two adjacent photonic bandgaps reported to date.

The proposed analytical description is consistent with the experimental results. It can be efficiently applied to design new hybrid PCFs and/or photonic bandgap fibers to develop wavelength converters and power exchangers and enhance the supercontinuum generation, which is based on many nonlinear effects such as dispersive wave emission [11].

Acknowledgments

This work was supported by CNPq, FAPEMIG, FINATEL, CAPES, MCTI and Prysmian-Draka. The authors thank J. Knight and A. George from University of Bath for their help during the fiber fabrication.

References

[1] S. Arismar Cerqueira Jr., Recent progress and novel applications of photonic crystal fibers, Rep. Prog. Phys. 73 (2010) 024401.
[2] S. Arismar Cerqueira Jr., F. Luan, C.M.B. Cordeiro, A.K. George, J.C. Knight, Hybrid photonic crystal fiber, Opt. Express 14 (2006) 926–931.

[3] L. Xiao, W. Jin, M.S. Demokan, Photonic crystal fibers confining light by both index-guiding and bandgap-guiding: hybrid PCFs, Opt. Express 15 (2007) 15637–15647.
[4] Yacoub Ould-Agha, Aurelie Bétourné, Olivier Vanvincq, Géraud Bouwmans, Yves Quiquempois, Broadband bandgap guidance and mode filtering in radially hybrid photonic crystal fiber, Opt. Express 20 (2012) 6746–6760.
[5] S. Arismar Cerqueira Jr., D.G. Lona, I. de Oliveira, H.E. Hernandez-Figueroa, H.L. Fragnito, Broadband single-polarization guidance in hybrid photonic crystal fibers, Opt. Lett. 36 (2011) 133–135.
[6] Thomas Tanggaard Alkeskjold, Large-mode-area ytterbium-doped fiber amplifier with distributed narrow spectral filtering and reduced bend sensitivity, Opt. Express 17 (2009) 16394–16405.
[7] M. Pang, L.M. Xiao, W. Jin, S. Arismar Cerqueira Jr., Birefringence of hybrid PCF and its sensitivity to strain and temperature, J. Lightwave Technol. 30 (2012) 1422–1432.
[8] A. Bétourné, A. Kudlinski, G. Bouwmans, O. Vanvincq, A. Mussot, Y. Quiquempois, Control of supercontinuum generation and soliton self-frequency shift in solid-core photonic bandgap fibers, Opt. Lett. 34 (2009) 3083–3085.
[9] S. Arismar Cerqueira Jr., Cristiano M.B. Cordeiro, F. Biancalana, P.J. Roberts, H.E. Hernandez-Figueroa, C.H. Brito Cruz, Nonlinear interaction between two different photonic bandgaps of a hybrid photonic crystal fiber, Opt. Lett. 33 (2008) 2080–2082.
[10] Vincent Pureur, John M. Dudley, Nonlinear spectral broadening of femtosecond pulses in solid-core photonic bandgap fibers, Opt. Lett. 35 (2010) 2813–2815.
[11] Dane R. Austin, C. Martijn de Sterke, Benjamin J. Eggleton, Thomas G. Brown, Dispersive wave blue-shift in supercontinuum generation, Opt. Express 14 (2006) 11997–12007.
[12] S. Arismar Cerqueira Jr., K.Z. Nobrega, H.E. Hernandez-Figueroa, F. Di Pasquale, PCFDT: an accurate and friendly photonic crystal fiber design tool, Optik 119 (2008) 723–732.
[13] Magnus Haakestad, Johannes Skaar, Causality and Kramers–Kronig relations for waveguides, Opt. Express 13 (2005) 9922–9934.
[14] Y. Kodama, A. Hasegawa, Nonlinear pulse propagation in a monomode dielectric guide, J. Quant. Electron. 23 (5) (1987) 510–524.
[15] G. Agrawal, Nonlinear Fiber Optics, Academic Press, 2013 (Chapter 12).
[16] A. Fuerbach, P. Steinvurzel, J. Bolger, B. Eggleton, Nonlinear pulse propagation at zero dispersion wavelength in anti-resonant photonic crystal fibers, Opt. Express 13 (2005) 2977–2987.
[17] A.V. Husakou, J. Herrmann, Supercontinuum generation of higher-order solitons by fission in photonic crystal fibers, Phys. Rev. Lett. 87 (2001) 203901.
[18] N. Akhmediev, M. Karlsson, Cherenkov radiation emitted by solitons in optical fibers, Phys. Rev. A 51 (1995) 2602–2607.
[19] S. Arismar Cerqueira Jr., A.R. do Nascimento Jr., M.A.R. Franco, I. de Oliveira, V.A. Serrão, H.L. Fragnito, Numerical and experimental analysis of polarization properties from hybrid PCFs across different photonic bandgaps, Opt. Fiber Technol. 18 (2012) 462–469.
[20] S. Arismar Cerqueira, A.R. do Nascimento Jr., M.A. Gouveia, C.M.B. Cordeiro, Efficient energy transfer between photonic bandgaps, in: Lasers and Electro-Optics (CLEO), 2012 Conference on, May 2012.